The 18.3% Silicon Solar Cells with Nano-Structured Surface and Rear Emitter *

Jun-Na Zhang(张军娜), Lei Wang(汪雷)**, Zhun Dai(戴准), Xun Tang(唐勋), You-Bo Liu(刘友博), De-Ren Yang(杨德仁)**

State Key Laboratory of Silicon Materials and School of Materials Science and Engineering, Zhejiang University, Hangzhou 310027

(Received 9 November 2016)

A nano-structured surface is formed on the pyramid structure of n-type silicon solar cells by size-controlled silver nano-particle assisted etching. Such a nano-structure creates a front average weighted reflectance of less than 2.5% in the 300–1200 nm range due to the broadband reflection suppression. The sodium hydroxide is used to obtain the low-area surface by post-etching the nano-structure, thus the severe carrier recombination associated with the nano-structured surface could be reduced. After emitter forming, screen printing and firing by means of the industrial fabrication protocol, an 18.3%-efficient nano-structured silicon solar cell with rear emitter is fabricated. The process of fabricating the solar cells matches well with industrial manufacture and shows promising prospects.

PACS: 88.40.jj, 81.65.Cf, 82.45.Yz, 84.60.Jt DOI: 10.1088/0256-307X/34/2/028801

For silicon (Si) solar cells, optical loss is one of the major obstacles to improve the conversion efficiency. In general, cell efficiency can be increased by means of reducing the reflectivity of Si wafers and maximizing the absorption of incident light. Some anti-reflective structures including the pyramid structure[1–3] have been used to provide beneficial light trapping for Si solar cells. However, the average reflectance of silicon solar cells after the current pyramid texture process, which is higher than 10% in the visible light scale, is still high. In the last decade, nano-structured surfaces of Si wafers, which were fabricated by reactive ion etching,[4–6] electrochemical etching,[7,8] metal-assisted etching[9–13] and so on, have been widely investigated for their prominent light-trapping feature. Among them, metal-assisted chemical etching is favorable for industrial applications, as it overcomes the disadvantage of the dry etch technique which needs either complicated fabricating processes and expensive instruments or high energy consumption. Recently, some metal-assisted chemical etching methods to fabricate nanostructures on the surfaces of silicon solar cells have been reported by our group,[14,15] and the lowest average reflectance is ∼5%.

Although nano-structured Si solar cells exhibit high absorption over a wide spectral range, they show poor efficiency compared with current commercial silicon solar cells. Since noble metals as the catalyst for etching could have survived on the surface of wafers after the fabrication of nanostructures, they could diffuse to the p–n junction, resulting in electron shunting or forming minor carrier recombination centers in the subsequent process of heat treatments. Meanwhile, the surface area is increased significantly due to the formation of nanostructures, and then the photo-carrier recombination is dramatically enhanced, leading to a decline of the short-circuit current of nano-structured silicon solar cells. To avoid the latter problem, the post-etching method is generally used to reduce the recombination of a nano-structured surface. For example, a nano-structured silicon solar cell with higher efficiency was achieved by reducing carrier recombination using tetramethylammonium hydroxide (TMAH) to post-etch the nanostructures so as to control the final surface morphologies and areas.[16] There are reports that the α-Si:H/SiN$_x$ stack-layer films prepared by plasma-enhanced chemical vapor deposition can also be used to passivate the crystalline silicon solar cells to reduce the surface carrier recombination.[17]

Among those previous reports, nano-structured surfaces are mostly formed on p-type solar grade Si wafers. In fact, the minority carrier lifetime of p-type Si wafers is usually shorter than that of n-type Si wafers,[18] as the minority carrier lifetime can be reduced by boron-oxygen complexes acted as recombination centers.[19] Therefore, n-type silicon wafers are generally chosen for fabrication of high efficiency solar cells. Among the n-type solar cells, a rear emitter cell structure is a promising way to increase the cells' conversion efficiency when the metal-assisted texture method is adopted.[20] As mentioned before, the residual novel metal is harmful for cells. The rear emitter solar cells with a deep p–n junction can avoid the detriment of residual novel metal. Thus the internal quantum efficiency can be increased and higher conversion efficiency can be achieved.

In this Letter, a new black silicon n-type solar cell with rear emitter is proposed to include nano-

*Supported by the National Natural Science Foundation of China under Grant No 51532007, the Major Projects of Zhejiang Province under Grant No 2013C01037, and the Foundation of State Key Lab of Silicon Materials.

**Corresponding author. Email: phy_wangl@zju.edu.cn; mseyang@zju.edu.cn

© 2017 Chinese Physical Society and IOP Publishing Ltd

structured front surfaces with post-etch treatment, phosphorus and boron diffusion, respectively, on the front and rear sides. Such nano-structured silicon solar cells with rear emitter could effectively avoid the detriment of surviving noble metal on the surface to rear p–n junction. Finally, 15.6 cm×15.6 cm n^+np rear emitter solar cells with the conversion efficiency of 18.3% are obtained.

The fabrication process of the n^+np nano-structured silicon solar cells with a rear emitter is schematically shown in Fig. 1. Firstly, a pyramid structure is formed on the surface of an n-type Si wafer, and then Ag nano-particles (NPs) are deposited on the pyramidal structured silicon surfaces. Then, the nano-structure on the pyramid structure of wafers is obtained by etching with Ag NPs assisted. Later, NaOH is used to post-etch the nano-structure to broaden the nano-holes and to reduce the depth of nanostructures. Moreover, unsound silicon dioxide (SiO_2) layers on nano-structured surfaces are also removed by NaOH. Followed by the industry process, the front n^+ layer is formed through phosphorus diffusion, the rear emitter (the p layer) is formed through boron diffusion and silicon nitride (SiN_x) antireflection layers are grown on the front surface via plasma enhanced chemical vapor deposition (PECVD). Subsequently, the metal (Ag) as electrical contacts is printed via the screen-printing on the front and rear surfaces. After firing, the n^+np nano-structured silicon solar cells are eventually obtained. This whole process is a simple and low-cost way to fabricate high efficiency nano-structured silicon solar cells.

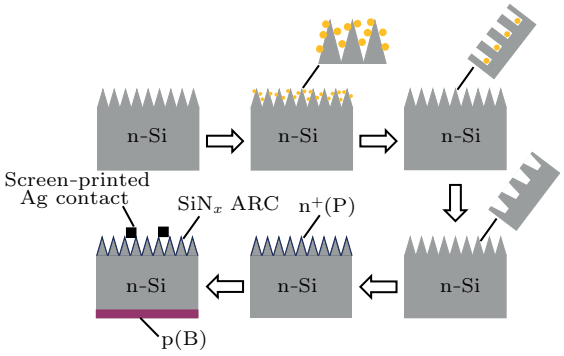


Fig. 1. Schematic manufacturing process of nano-structured silicon solar cells.

According to the method of synthesizing the size-controlled colloidal Ag NPs reported by our group,[21] Ag NPs were prepared firstly. Simply, a formaldehyde solution (CH_2O, 37 vol%) was added into silver nitrate ($AgNO_3$, 0.1 mol/L) at 35℃, and the ammonium hydroxide ($NH_3{\cdot}H_2O$, 28 vol%) was injected immediately to initiate the reaction using the polyvinylpyrrolidone (PVP) as a surfactant. The reaction mixture was stirred for 30 min before centrifugation.

The n-type solar grade C_z (100) silicon wafers (1–10 Ω·cm, 15.6 cm×15.6 cm) were purchased from the Zhejiang Jin Bei Energy Science and Technology Co., Ltd. Wafers were put into the mixture of 3 wt% potassium hydroxide solution (KOH) and isopropyl alcohol solution (IPA, 7 vol%) at 80℃ for 60 min to fabricate the pyramid structures after being cleaned by 20 wt% KOH at 80℃ for 2 min to remove saw damage. Then, the Si wafers were immersed into the deionized water (DIW) containing dispersed Ag NPs, while their rear surfaces were protected and separated from the Ag NPs. After keeping the solution evaporating in the atmosphere to make Ag NPs firmly fix on the Si wafers surfaces, the wafers were put into the mixture solution of HF:H_2O_2:DIW=1:5:10 (vol) in the light-proof container in different durations (3–6 min), and nano-structured surfaces on the pyramid structure of Si wafers were obtained. The remanent Ag NPs were removed by a salpeter solution (HNO_3, 65 wt%) and the wafers were rinsed by DIW. Later, 2 wt% NaOH was used to post-etch nanostructures for 3 min, then the wafers were immersed into hydrochloric acid (HCl, 10 vol%) and DIW to remove the sodium existing on the surfaces of Si wafers. Finally, followed by the industrial process, nano-structured solar cells with a rear emitter have been fabricated.

The morphology and structures of the samples were characterized by a field emission scanning electron microscope (FESEM Hitachi U-70). Reflectance spectra of the Si wafers surfaces were tested using a spectrometer (Hitachi U-4100 Spectrophotometer) with an integrating sphere. The effective carrier lifetime distribution images of these samples were characterized by a microwave photoconductance decay technique (WT-2000mPCD, Semilab). Solar cell efficiency was tested under AM 1.5 G spectral irradiance (100 mW/cm^2 at 25℃) by a BERGER Lichttechnik Single Cell Tester.

Ag NPs with the size in the range of 50–60 nm were obtained through control of the reaction parameters. It can be found that the particles are spherical and show a narrow size-distribution. After the fabrication of the nano-structure on the pyramid surface of wafers, Ag NPs acting as a catalyst should be removed by NaOH cleaning. However, there might still be residual Ag NPs existing on the nanostructures, which may diffuse to the p–n junction, resulting in electron shunting or forming minor carrier recombination centers. The solar cell with the rear emitter proposed in this work, i.e., fabricating a deep n–p junction, could reduce the diffusion length and could decrease the bad influence.

Figure 2 compares scanning electron microscopy (SEM) images of the Si wafers after Ag NPs-assisted etching for different times. Figure 2(a) displays the pyramid structure of Si wafers without nanostructures, i.e., before the etching. Figures 2(b)–2(d) show

the nanostructures on the pyramid structure of Si wafers etched for 4 min, 5 min and 6 min. It can be seen that numerous nanopores are distributed uniformly on the pyramidal structure, and the depth of the nanopores L increases with the etching time. A refractive index gradient is formed between air and Si wafers through fabricating the nanopores on the pyramid surfaces of the Si wafers, which could suppress surface reflection.[22]

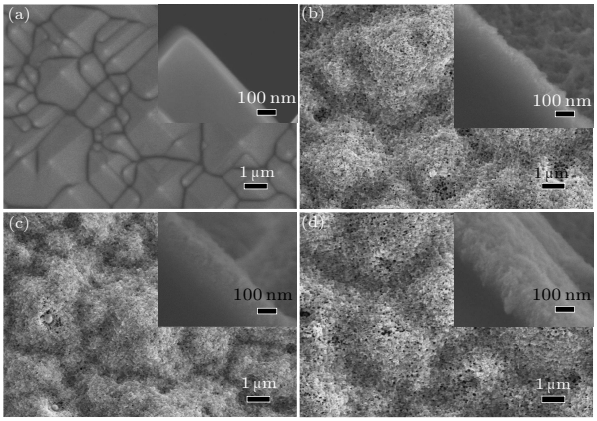


Fig. 2. SEM images of the morphology of Si wafer surfaces and the depth of the nanopores (L) for different etching times with Ag NPs assisted etching: (a) before etching (original), (b) 4 min, (c) 5 min, and (d) 6 min. The insets are the cross section SEM images of the respective wafers.

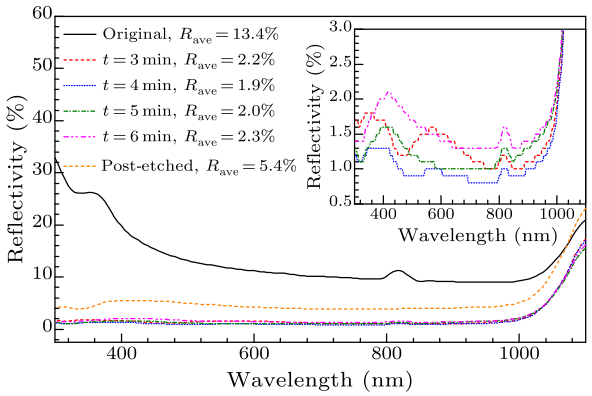


Fig. 3. Reflectance spectra of the Si wafer surfaces and the average reflectance (R_{ave}). The inset is the detail reflectance information of nano-structured Si wafers for different etching times.

The average reflectance values would be different as the etching time varies. Figure 3 shows the reflectance ($R(\lambda)$) spectra of the nano-structured Si wafers for different etching times. It can be seen that $R(\lambda)$ of nano-structured Si wafer surfaces is much lower than that of pyramid structured Si wafer surfaces without the etching. After a series of experiments, the average reflectance R_{ave} could be achieved below 2.4% when the etching time varies from 3 min to 6 min, and the lowest average reflectance is 1.9% when the Si wafers are etched for 4 min.

The reflectance spectra of Si wafers would also be influenced by post-etching. As shown in Fig. 3, R_{ave} of the silicon surface reduced from 13.4% to 1.9% due to the formation of the nano-structure on the pyramid surface of the Si wafer, while it increases to 5.4% after NaOH post-etching. Compared with the wafers with the pyramidal structure, $R(\lambda)$ of the wafers with the post-etched nano-structure is still much lower.

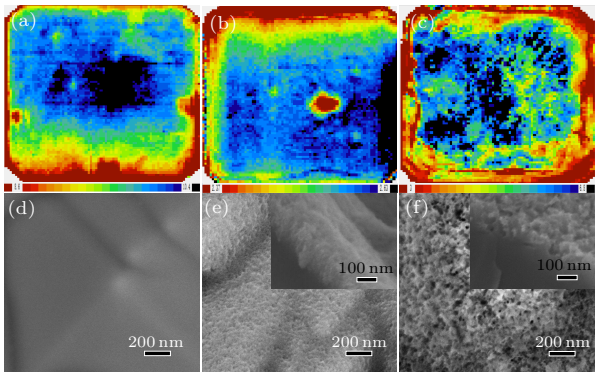


Fig. 4. The effective minority carrier lifetime distribution graphs of the n-type silicon wafers and their corresponding SEM images: (a, d) the Si wafer without Ag NPs assisted etching, (b, e) Si wafer with Ag NPs assisted etching, and (c, f) Si wafer with Ag NPs assisted etching and post-etching by NaOH.

Photocarrier recombination on the surface area of nano-structured Si wafers significantly increases, thus the short-circuit current (J_{SC}) and open circuit voltage (V_{OC}) of solar cells would be reduced.[14] To reduce the photocarrier recombination, NaOH was selected in our experiments to post-etch the nanostructure surfaces to remove the unsound SiO_2 layers. Figures 4(a)–4(f) display the minority carrier lifetime distribution graphs of the Si wafers with pyramidal structure, nano-structure and post-etched nanostructure, as well as their corresponding microstructure images (downside), respectively. The average effective minority carrier lifetime decreases from 9.6 μs to 2.5 μs when nano-structured surfaces are formed on the Si wafer, because of stronger minority carrier recombination. Through post-etching by NaOH, the average effective minority lifetime of the nanostructured Si wafer increases to 5.1 μs because the photocarrier recombination on the nanostructures is weakened, and the nanopores diameter becomes larger and the depth of pores appears to be shallower. It can be seen that the average depth of the nanopores in the Si wafers with nano-structured surfaces has been decreased to about 110 nm. It is clear that the post-etched nanostructures have lower surface area, leading to less carrier recombination on the surface. Thus with lower reflectivity and higher minority carrier lifetime, J_{SC} of post-etched nano-structured solar cells will increase and the higher cell efficiency will be achieved.

The post-etched nano-structured surfaces weaken

the surface recombination and increase V_{oc} and J_{SC} despite reducing the absorption slightly. In Table 1, the PNCz-Si cell shows an 18.3% efficiency with $V_{oc} = 637.64\,\text{mV}$, $J_{sc} = 37.43\,\text{mA/cm}^2$ and $FF = 76.61\%$, while the efficiency of NCz-Si cell without post-etching is 15.9%. It is obvious that after the post-etching, J_{SC} is increased by $3.82\,\text{mA/cm}^2$ and the efficiency is increased by 2.4% because of the higher minority carrier lifetime and reduced recombination.

Table 1. Efficiency and I–V parameters of the silicon solar cells of the nano-structured Cz silicon solar cell (NCz-Si cell) and the post-etched nano-structured Cz silicon solar cell (PNCz-Si cell).

Sample	V_{oc} (mV)	J_{sc} (mA/cm^2)	FF (%)	η (%)
NCz-Si cell	616.17	33.71	76.37	15.9
PNCz-Si cell	637.64	37.43	76.61	18.3

In summary, we have used $15.6\,\text{cm} \times 15.6\,\text{cm}$ n-type Cz Si wafers to fabricate rear emitter solar cells. By forming nanostructures on the pyramid surfaces of Si wafers through Ag NPs assisted etching, relatively low reflectivity (a minimum of 1.9%) of Si wafers is obtained. Because of serious surface recombination, the efficiency of the nano-structured silicon solar cell is only 15.9%. However, after NaOH post-etching, the surface recombination is reduced and a relatively low reflectivity is retained. Finally, an 18.3%-efficient nano-structured silicon solar cell is achieved. It is suggested that this nano-structured silicon solar cell with rear emitter is very prospective for practical applications in the photovoltaic industry, and the process of fabricating the nano-structured silicon cell is very simple. Moreover, the efficiency has great potential to be further improved by optimizing alkali post-etching, choosing reasonable passivation and fabricating more shallow rear junctions. This method matches very well with the current commercially industrial craft of solar cells and has broad application prospects.

References

[1] Cheng H H, Chang Y Y, Chu J Y et al 2012 *Appl. Phys. Lett.* **101** 141113
[2] Singh P K, Kumar R, Lal M et al 2001 *Sol. Energy Mater. Sol. Cells* **70** 103
[3] Dimitrov D Z and Du C H 2013 *Appl. Surf. Sci.* **266** 1
[4] Khuat V, Ma Y C, Si J H et al 2014 *Chin. Phys. Lett.* **31** 037901
[5] Li T, Zhou C L, Wang W J 2016 *Chin. Phys. Lett.* **33** 038801
[6] Otto M, Kroll M, Käsebier T et al 2010 *Adv. Mater.* **22** 5035
[7] Marrero N, Guerrero L R, González D B et al 2009 *Thin Solid Films* **517** 2648
[8] Ge J, Yin W J, Long Y F et al 2007 *Chin. Phys. Lett.* **24** 1361
[9] Li X and Bohn P W 2000 *Appl. Phys. Lett.* **77** 2572
[10] Peng K and Zhu J 2004 *Electrochim. Acta* **49** 2563
[11] Gu X, Yu X G, Liu T et al 2011 *Nanotechnology* **22** 025703
[12] Chartier C, Bastide S and Lévy-Clément C 2008 *Electrochim. Acta* **53** 5509
[13] Srivastava S K, Kumar D, Vandana et al 2012 *Sol. Energy Mater. Sol. Cells* **100** 33
[14] Xiao J F, Wang L, Li X et al 2010 *Appl. Surf. Sci.* **257** 472
[15] Li D, Wang L, Li D S et al 2013 *Appl. Surf. Sci.* **264** 621
[16] Oh J, Yuan H C and Branz H M 2012 *Nat. Nanotechnol.* **7** 743
[17] Zheng X, Yu X G and Yang D R 2013 *Acta Phys. Sin.* **62** 198801 (in Chinese)
[18] Cuevas A, Kerr M J, Samundsett C et al 2002 *Appl. Phys. Lett.* **81** 4952
[19] Schmidt J, Bothe K, Bock R et al 2007 *22nd European Photovoltaic Solar Energy Conference* (Milan, Italy 3–7 September 2007) p 998
[20] Fertig F, Wöhrle N, Greulich J et al 2016 *Prog. Photovoltaics* **24** 818
[21] Liu T, Li D, Yang D et al 2011 *Mater. Lett.* **65** 628
[22] Branz H M, Yost V E, Ward S et al 2009 *Appl. Phys. Lett.* **94** 231121